

Influence of tool geometry for FSW on weldability of AW7075-T651 alloy

Jozef Bárta^{1*}, Ján Urminský¹, Lukáš Válek¹, Katarína Bártová¹, Milan Marônek¹, and František Jurina¹

¹Slovak University of Technology in Bratislava, Faculty of Materials Science and Technology in Tmava, Slovakia

Abstract. Nowadays, there is a strong effort to take ecological aspects into account in industrial applications. One of these applications is welding, where friction is one of the best ways to lower waste material in production. This technology is clean with no fumes, harmful radiation, or manual skill required as it is fully automated. The paper deals with the effect of five different tool geometries for friction stir welding on weld joint structural properties. The probe of the tool used in this experiment was in the shape of a threaded cone cut into a regular pyramid (3-, 4- and 5-sided). The shoulder had a triple helix-shaped groove with 0.5 mm depth. To evaluate the influence of the size of pyramid versus size of thread, three different sizes of four-sided pyramid were used. X-ray analysis revealed the porosity in the case of two probes. Even though 4-sided pyramid showed the best performance during the welding, all probes succeeded to provide a good quality weld with using different welding parameters. Structural analysis of weld joints revealed the presence of standard zones (HAZ, TMAZ and SZ). The size of the grains in stir zone varied from 2 to 5 μm .

1 Introduction

Friction stir welding was invented at the end of the 20th century by TWI in Cambridge [1].

Its domain is that the welding process takes place at temperatures lower than the melting temperature of the basic materials. Therefore, it is a solid-state joining method of materials. FSW can be extensively applied to a variety of materials, including aluminium, copper and magnesium alloys. The welding temperature is closely related to the melting temperature of the welded materials. The welding temperature usually ranges from 0.6 to 0.8 of the melting temperature [2]. Nowadays, friction stir welding is mostly used in the automotive, aviation, marine, shipbuilding industries and other industries. In the automotive industry, FSW is used for welding bodies, frames and engine components and currently battery boxes as well [3].

Compared to traditional arc welding methods, FSW has several advantages. Defects such as pores and cracks related to solidification of the material during welding are excluded. However, defects typical of FSW can be created during welding, such as a tunnel defect and so on [4,5].

The principle of FSW utilizes a specially designed tool consisting of a shoulder and a probe. The tool is pressed into the material, followed by plasticization of the material caused by the heat from friction. Subsequent movement of the tool along the welding edge between the two materials starts the welding process. At the end of welding, the tool emerges from the material [6,7].

Friction stir welding has a limited number of process parameters, which are divided into machine- and tool-related factors that control the quality of the weld and the various mechanical properties of the welded material. In Figure 1 the various parameters and variables of the FSW process are shown. Tool rotation speed, tool movement rate, axial load or plunging force and tool inclination angle are machine related

parameters. Shoulder diameter, probe length and probe geometry are just a few characteristics of the welding tool. The quality of the weld joint can be affected by controlling these variables [5]. Two process parameters, tool speed and welding speed, have a significant influence on weld joint quality [5,8].

Light aluminum alloys are irreplaceable materials in many engineering fields, mainly in transport and construction [9]. With the help of friction stir welding, it is possible to make high-quality welds from alloys of the 7xxx series, which are considered difficult to be welded using classic welding methods. Calculation of heat input is important in fusion welding. In the FSW method, welding current and voltage are not present and these quantities are replaced by friction, rotation and applied force. The heat input is mechanical. Several studies have been carried out to identify the ways in which heat is generated and transferred to the joint area, a simplified model of heat input can be given as follows:

$$Q = \mu \cdot \omega \cdot F \cdot K \quad (1)$$

where, heat (Q) is the product of friction (μ), tool rotation speed (ω), pressure force (F) and tool geometry constant K [10]. It is the geometry of the tool that affects the amount of generated heat input in the welding process, and based on the heat input, it is possible to influence the resulting quality of the weld joints. The flow of the plasticized material is influenced by the geometry of the tool but also by the welding speed and the speed of rotation of the tool. The diameter of the shoulder is important because the shoulder generates most of the heat. The geometry of the probe affects the material flow and the resulting properties of the weld joint [8]. When welding aluminum alloys, the wear of the welding tool is not so significant, and tool steel can be used to make the tool [3]. Friction stir welding does

* Corresponding author: jozef.barta@stuba.sk

not have negative effects on the environment compared to other technologies because it minimizes harmful fumes and emissions [1,4,12].

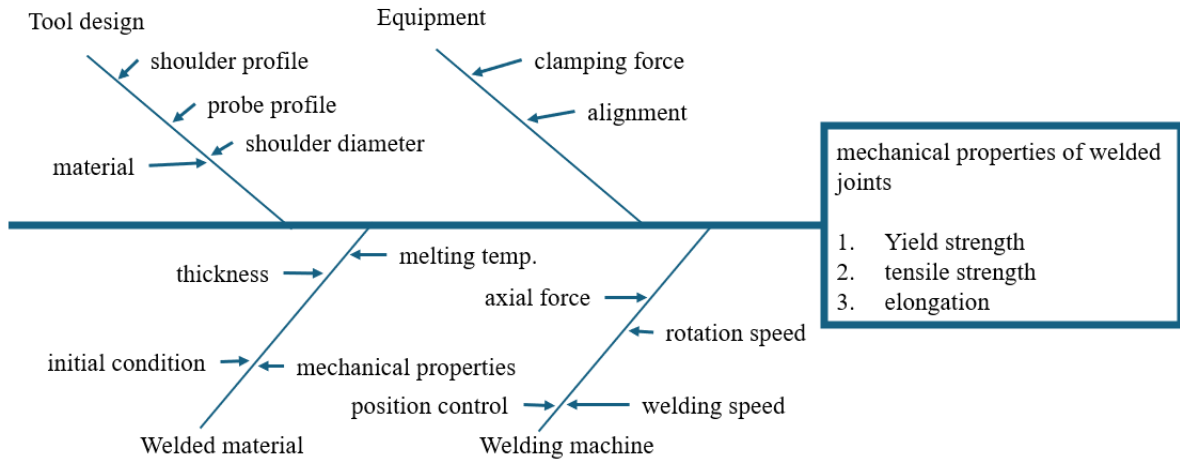


Fig. 1 Fishbone diagram with welding parameters [5]

2 Materials and methods

Aluminum alloy AW7075-T651 with a thickness of 5 mm was used in the experiment. The chemical composition and mechanical properties of AW7075-T651 are shown in Table 1 and Table 2. The chemical composition was analyzed using Bruker Q4 TASMAN optical emission spectrometer.

Table 1. Chemical composition of AW7075-T651 [wt. %]

Al	Cr	Cu	Fe	Mg
88.7	0.178	1.740	0.201	2.511
Mn	Si	Ti	Zn	iné
0.059	0.082	0.018	6.440	0,071

Table 2. Typical mechanical properties of AW7075-T651 [9]

Hardness, Brinell	150	AA; Typical; 500 g; 10 mm ball
Hardness, Rockwell B	87	Calculated from Brinell
Hardness, Vickers	175	Calculated from Brinell
Tensile strength	538 MPa	AA; Typical
Yield strength	476 MPa	AA; Typical

Different probe geometries and only one geometry of shoulder were used during welding. The design of the geometry was based on the knowledge obtained from the literature review and 5 different probe geometries were used (Figure 3). The tip of the tool had the shape of a cone cut into a regular pyramid with a different number of sides, with a thread. The length of the tip of the tools was 4.9 mm and the diameter of the tip was 5.5 mm. The arm diameter was 14 mm and there were 3 grooves in the shape of a helix with a depth of 0.5 mm

on the contact surface of shoulder (Figure 2). The shoulder was made of H13 tool steel and the tool tip was tungsten carbide.

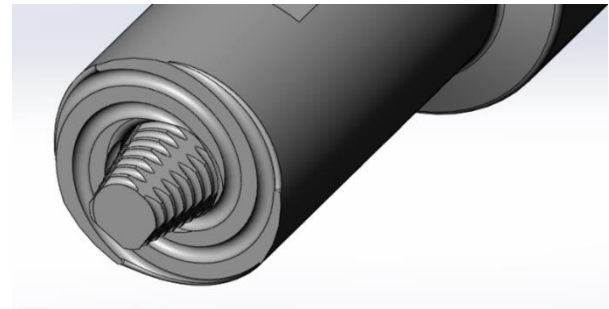


Fig. 2 Tool design in 3D view

The welds were produced on the DMU 85 monoBLOCK (5-Axis Milling machine from DMG MORI), which is a standard milling machine. Based on previous experiments, the same welding parameters were chosen for all tool geometries. The welding parameters are listed in Table 3. It was assumed that by changing the geometry of the pin used during the welding process, different heat is generated, which is necessary to produce the welded joint. Changing the geometry of the probe also results in a change in the degree of mixing of the welded material.

Table 3. Welding parameters

Revolution frequency	1000 min ⁻¹
Welding speed	600 mm.min ⁻¹
Shoulder penetration into the material	0,1 až 0,2 mm
Tool angle	0°
Number of geometries	5

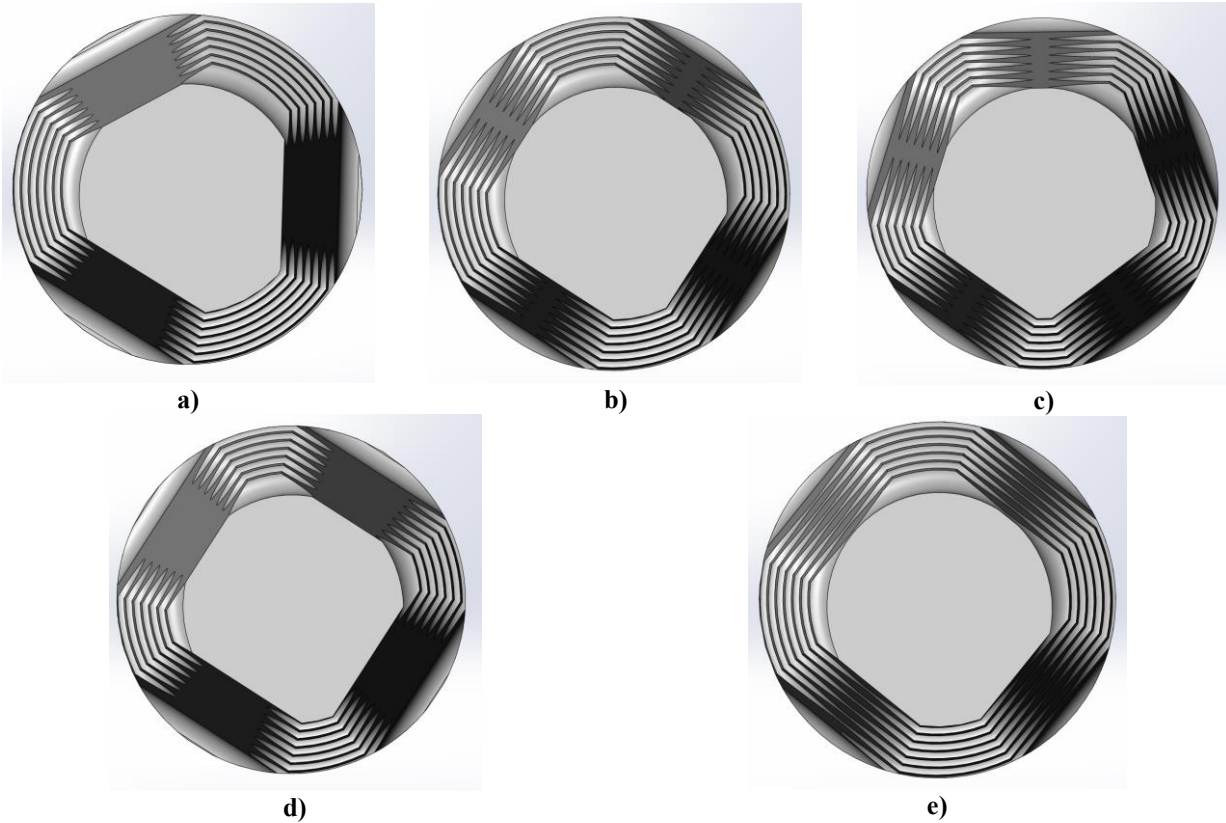


Fig. 3 Probe geometries (top view); a) 3HR - truncated triangular pyramid with thread; b) 4HR - truncated quadrilateral pyramid with thread; c) 5HR - truncated pentagonal pyramid with thread; d) 4HR-HI - truncated quadrilateral pyramid with a thread and a deeper grinded surface; e) 4HR-LO - truncated quadrilateral pyramid with a thread and a shallower grinded surface

The manufactured samples were inspected for internal defects using CT X-Ray device and the structure of the weld joint was evaluated using metallography. CT X-ray analysis was performed on a ZEISS Metrotom 1500, and VG Studio 3.0 software was used to evaluate the obtained X-ray scans. Structural analysis was carried out using standard procedures. After grinding and polishing, Keller's reagent (95 mL H₂O, 2.5 mL HNO₃, 1.5 HCl, 1 mL HF) was used to develop the macrostructure and microstructure of the weld joints.

3 Results

The samples were marked according to Figure 3. Visual inspection was carried out on all five weld joints and the shape of the weld joints in the cross-section was observed to evaluate the microstructure. Prior to structural analysis, the weld joints were evaluated for the presence of internal defects. The samples were subjected to volumetric analysis. Based on the CT X-ray analysis, it can be concluded that only one tool, in this case a truncated pentagonal pyramid with a thread (5HR), had a systematically recurring defect. Specifically in the root part of the weld, there was a gradual formation of a tunnel defect observed (Figure 4). The tool plunge cavity observed with the 3HR, 4HR-LO and 4HR-HI tools can be avoided by adjusting the tool plunge rate.

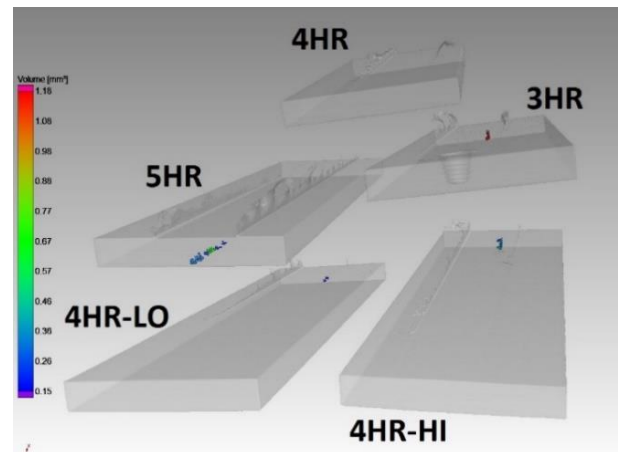


Fig. 4 Result of CT X-Ray analysis

Tables 4 and 5 document the surfaces of the weld joints and their cross-section. No external defects were observed on the surface or in the root of the weld. In root part of the weld, it was possible to observe a heat-affected area, the width of which was constant along the entire length of the weld. The surface of the weld joints shows a drawing specific to the shoulder of welding tool. There was a flash on all the welded joints, which did not have any effect on the conditions of the evaluation of the experiment. Size of the flash is adequate to the penetration of the tool into the material. By analyzing the shape of weld joint in the cross-section, it is possible to accurately determine the individual zones of the weld joint typical for the FSW

method, specifically the stir zone (SZ), the thermomechanically affected zone (TMAZ), the heat affected area (HAZ) and the base material (BM).

Table 4. Weld surface appearance






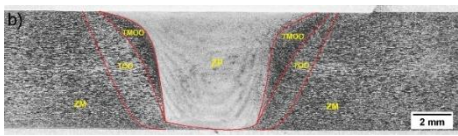
Marking	Weld joint surface
3HR	
4HR	
5HR	
4HR-HI	
4HR-LO	

Table 5. Analysis of weld joint shape in cross-section

Marking	Macrostructure of the weld joint
3HR	

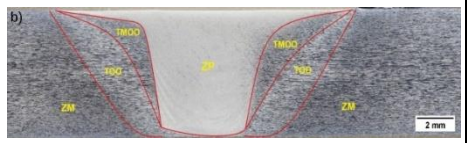
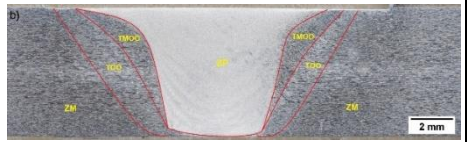
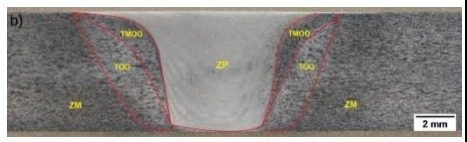
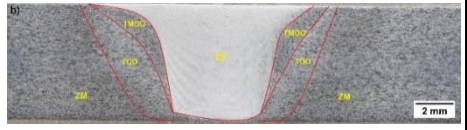
Marking	Macrostructure of the weld joint
4HR	
5HR	
4HR-HI	
4HR-LO	

Figure 5 documents the transition zone of sample 3HR, with stir zone from the left side. The thermomechanically affected zone is very significant, especially in the area closer to the surface of the weld joint, as in this area the heat input is the most significant, combining the heat generated by the probe as well as the tool shoulder. The macrostructure of the weld joints did not show the presence of defects in the weld joint.

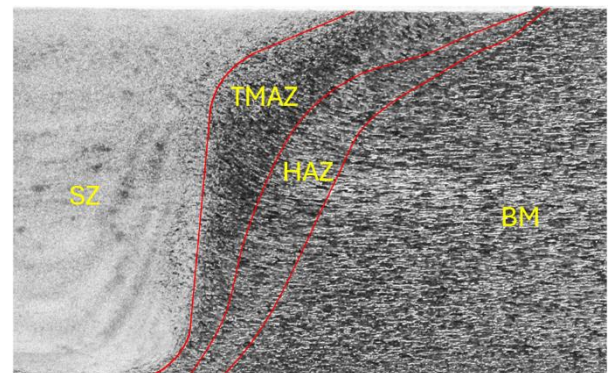


Fig. 5 Detail of transition zone of sample 3HR

The microstructure is documented only on the 3HR sample, as the transition areas as well as the structures are very similar and differ mainly in the shape and size of the individual zones of the weld joint. Figure 6 documents the microstructure of the weld metal in the stir zone. The structure of the weld metal was formed by polyhedral grains with an average grain size of about 4 μm .

A sharp transition from the weld metal to the thermomechanically affected zone was observed (Figure 7). The thermomechanically affected zone is characterized by significant deformation of columnar grains. Secondary particles were documented inside of columnar grains (probably precipitates from the original structure of the material).

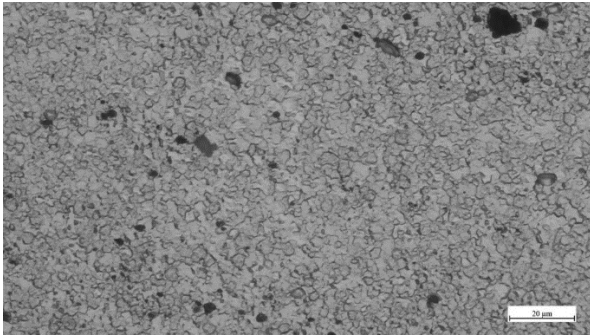


Fig. 6 Stir zone of sample 3HR

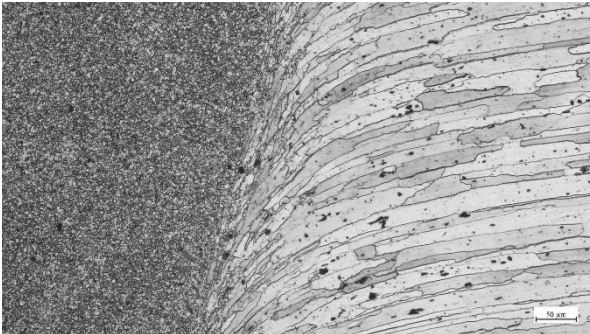


Fig. 7 Transition of stir zone to TMAZ on advancing side of sample 3HR

4 Conclusions

All the designed geometries were able to produce a satisfactory weld joint using given welding parameters, except for the 5HR tool, where a systematic error was observed in the root of the weld joint. Several tools had a positive cavity identification early in the process that can be removed by simply adjusting the plunge rate.

The weld joints showed standard zones such as heat affected zone, thermomechanically affected zone and mixing zone. The weld metal was formed by a fine-grained polyhedral structure with a grain size of approximately 4 μm. Tool 4HR produced a weld joint with no defect observed inside or on the surface of the weld joint.

The defined geometries of the tool did not bring significant differences in the geometry of the weld joint or in the microstructure of the weld joint. It can be concluded that the size of grinded surfaces of the truncated pyramid as well as the number of their sides (at a given size of the probe) as a change in the geometry is not significant enough to be manifested by difference in weld joints shape or in defect formation.

Acknowledgements

This work was supported by Slovak Research and Development Agency under the contract No. APVV-21-0111.

References

- Kallee, S.W., Nicholas, E.D. and Thomas, W.M. (2001) 'Friction Stir Welding- Invention, Innovations and Applications', 8th International Conference on Joints in Aluminium.
- Kilic, S., Ozturk, F. and Demirdogen, M.F. (2023) 'A comprehensive literature review on friction stir welding: Process parameters, joint integrity, and mechanical properties', *Journal of Engineering Research*. Available at: <https://doi.org/10.1016/j.jer.2023.09.005>.
- Bhardwaj, N. et al. (2019) 'Recent developments in friction stir welding and resulting industrial practices', *Advances in Materials and Processing Technologies*
- Anand, R. and Sridhar, V.G. (2020) 'Studies on process parameters and tool geometry selecting aspects of friction stir welding-A review', in *Materials Today: Proceedings*. Available at: <https://doi.org/10.1016/j.matpr.2019.12.042>.
- Devanathan, C. et al. (2022) 'Review of Joining Various Materials by FSW Process and Applications', *Annals of Dunarea de Jos University of Galati. Fascicle XII, Welding Equipment and Technology*, 33, pp. 75–88. Available at: <https://doi.org/10.35219/awet.2022.06>.
- El-Sayed, M.M. et al. (2021) 'Welding and processing of metallic materials by using friction stir technique: A review', *Journal of Advanced Joining Processes*, 3, p. 100059. Available at: <https://doi.org/10.1016/j.jajp.2021.100059>.
- Gebremlak, G. and Balkeshwar, S. (2020) 'Friction Stir Welding and its Applications: A Review', 26(11), pp. 682–705. Available at: https://www.researchgate.net/publication/345133110_Friction_Stir_Welding_and_its_Applications_A_Review.
- Rai, R. et al. (2011) 'Review: Friction stir welding tools', *Science and Technology of Welding and Joining*, 16(4), pp. 325–342. Available at: <https://doi.org/10.1179/1362171811Y.0000000023>.
- Ali Mehri, Amir Abdollah-zadeh, Sina Entesari, Tohid Saeid, Jing Tao Wang, The effects of friction stir welding on microstructure and formability of 7075-T6 sheet, *Results in Engineering*, Volume 18, (2023), 101041, ISSN 2590-1230, <https://doi.org/10.1016/j.rineng.2023.101041>. (<https://www.sciencedirect.com/science/article/pii/S2590123023001688>)
- Sarang Shah, S. Tosunoglu, *Friction Stir Welding: Current State of the Art and Future Prospects* Published (2012) *Engineering, Materials Science*, (<https://www.semanticscholar.org/paper/Friction-Stir-Welding%3A-Current-State-of-the-Art-and-Shah-Tosunoglu/be3d521b796f9bce7edf3ebe98ead9d78172fd34>)
- Sudzanayi Chiteka, Friction Stir Welding/Processing Tool Materials and Selection, *International Journal of Engineering Reserch & Technology (IJERT)*, Vol. 2 Issue 11, (2013), ISSN 2278-0181
- El-Sayed, M.M. et al. (2021) 'Welding and processing of metallic materials by using friction stir technique: A review', *Journal of Advanced Joining Processes*, 3, p. 100059. Available at: <https://doi.org/10.1016/j.jajp.2021.100059>.